44th AIAA Aerospace Sciences Meeting and Exhibit
9 - 12 January 2006, Reno, Nevada

AIAA Paper 2006-0740

Extinction of Opposed-Flow Hydrocarbon Diffusion Flames by Chemically-Passive Suppressants at Normal and EVA Atmosphere Conditions

Khaled M. Shebl*, Ammar M. Abdilghanie†, Werner J.A. Dahm‡ and Gerard M. Faeth§
The University of Michigan, Ann Arbor, MI, 48109-2140, USA

The critical flame extinction strain rates of opposed-flow hydrocarbon diffusion flames in the presence of various chemically-passive fire suppressants were experimentally and computationally determined. The objective was to extend an earlier study of chemically-passive suppressant effectiveness at normal-atmosphere conditions to the EVA-atmosphere conditions used in spacecraft prior to external vehicular activity. Extinction strain rates were determined for fuel streams consisting of pure CH_4, C_2H_6, C_3H_8 or C_2H_4 and oxidizer streams composed of air with 0-30% volume fractions of Ar, N_2 or CO_2 as inert suppressants. For both normal and EVA atmospheres, the relative suppressant effectiveness increased in order from Ar to N_2 to CO_2. This ordering is consistent with the simple increase in specific heat produced by the suppressant concentration in a stoichiometric mixture of the fuel and oxidizer. The internal structure of C_2H_6 flames with and without each suppressant in normal and EVA atmospheres was examined using OPPDIF calculations to identify the mechanisms that determine the relative effectiveness of each suppressant. At any given suppressant concentration, peak flame temperature and maximum concentrations of OH, H and O radicals are higher in the EVA atmosphere than in normal atmosphere, consistent with the higher oxygen concentration under EVA conditions. This suggests that similar correlations as have been found at normal atmosphere for critical flame extinction strain rates with these parameters may govern suppressant effectiveness in the EVA atmosphere, allowing effectiveness of other suppressants at other atmospheric preparations to be inferred from these results. Results to date suggest that, due to the higher oxygen concentrations in the EVA atmosphere, the critical flame extinction strain rates are slightly higher in the EVA atmosphere than in a normal atmosphere.

Nomenclature

Symbols:

a_q	=	critical flame extinction strain rate
a_{q0}	=	extinction strain rate at zero suppressant concentration
B	=	pre-exponential factor in Arrhenius equation
C_p	=	heat capacity
M_i	=	molecular weight of species i
T	=	temperature
$T_u(Z)$	=	frozen temperature distribution $T_2 + Z(T_1 - T_2)$
T_a	=	activation temperature = E/R (activation energy/gas constant)
T_{st}	=	adiabatic flame temperature
Y_i	=	mass fraction of species i
Z	=	mixture fraction $Z_F/Y_{F,1}$
Z_{st}	=	stoichiometric mixture fraction
$(-\Delta h)$	=	heat of reaction

* Visiting Assistant Professor, Department of Aerospace Engineering, 1320 Beal Avenue, Ann Arbor, MI.
† Graduate Student Research Assistant, Department of Aerospace Engineering, 1320 Beal Avenue, Ann Arbor, MI.
‡ Professor and Head, Laboratory for Turbulence & Combustion (LTC), Department of Aerospace Engineering, 1320 Beal Avenue, Ann Arbor, MI. Fellow AIAA. Corresponding author.
§ Professor, Department of Aerospace Engineering, 1320 Beal Avenue, Ann Arbor, MI.

ν_F = moles of fuel reacting with the oxidizer
ν_O = moles of oxidizer reacting with the fuel
ρ = density
τ = $(T_2 - T_1) / (T_{st} - T_u(Z_{st}))$

Subscripts:

F = fuel
O = oxidizer
st = conditions at stoichiometric mixture fraction $Z = Z_{st}$
1 = conditions at fuel stream exit
2 = conditions at oxidizer stream exit

I. Introduction

DEVELOPMENT of effective fire-suppression systems is of particular importance for spacecraft fire safety. In terrestrial fire-suppression systems, chemically-active agents such as Halon 1301 (CF_3Br) have long been known to be highly effective[1-4], however in a closed spacecraft environment the reaction products which such agents generate can be dangerous to health and life-support systems[5,6]. For this reason, there has been considerable interest in understanding the relative effectiveness of various alternative chemically-passive fire suppressants for possible use in spacecraft environments. The manned spacecraft environments in which these suppressants must function include both normal atmosphere conditions, consisting of 21% oxygen in nitrogen at 1 bar pressure, as well as EVA atmosphere conditions used in preparation for external vehicular activity, which consist of 30% oxygen in nitrogen at 0.7 bar pressure. Key interest is in understanding the effectiveness of various suppressant types on various fuel types in both these atmospheres, and in particular in developing insights into the fundamental mechanisms that determine the relative suppressant effectiveness. Such insights may allow identification of more effective chemically-passive fire suppressants, as well as identification of other suitable spacecraft atmospheres that provide for more effective fire safety. The present study thus investigates the relative effectiveness of the chemically-passive fire suppressants on extinction of hydrocarbon-air diffusion flames, as well as the structure of suppressed and unsuppressed diffusion flames at both normal and EVA atmosphere conditions.

Fundamental investigations of fire suppressants have previously been conducted in both premixed[7,8] and diffusion[9,10] flames, however these have primarily focused on effects of chemically-active fluorinated or brominated agents. By contrast, the present study uses a steady laminar opposed-flow diffusion flame configuration to investigate fundamental aspects associated with the effectiveness of chemically-passive suppressants on the critical extinction strain rate for several key hydrocarbon fuels burning in air. The opposed-flow diffusion flame allows measurements under carefully controllable conditions, as well as corresponding one-dimensional calculations of flame properties to assist in interpreting the resulting flame structure. There have been previous studies of laminar opposed-flow diffusion flames without suppressants which have shown that extinction can occur as a result of conductive heat losses from the reaction zone as the strain rate is increased[11-16]. Additionally, radiative heat losses from the reaction zone have also been shown to be a potential contributing factor in diffusion flame extinction. Furthermore, when the nominal strain rate is sufficiently low, buoyancy effects can produce additional strain that can lead to extinction[17]. In the present study, effects of buoyancy and radiation have been kept sufficiently small to allow investigation of the purely strain-induced extinction of opposed-flow diffusion flames in the presence of chemically-passive fire suppressants.

While most opposed-flow diffusion flames studies have focused on extinction of unsuppressed flames, several prior investigations have included limited results for the effects of inert diluents on the extinction limits of such flames. In particular, Milne et al.[9] and Ishizuka and Tsuji[18] together have shown that increasing concentrations of He, Ar, N_2 and CO_2 in the fuel or oxidizer stream act to reduce the peak flame temperature until an extinction limit is reached. Puri and Seshadri[19] examined the effect of N_2 dilution level on the extinction strain rates of methane-air and propane-air flames. Their results showed a large reduction in extinction strain rate as the N_2 dilution level was increased, but was not directed at different fuels and suppressants to identify the extinction strain rates and flame structure at both normal and EVA atmosphere conditions.

An earlier study[20] specifically investigated the effects of Ar, N_2 and CO_2 as chemically-passive monatomic (Ar), diatomic (N_2) and triatomic (CO_2) fire suppressants supplied at concentrations up to 30% by volume in air to

the oxidizer stream in a steady laminar opposed-flow diffusion flame. Extinction strain rates were experimentally measured for fuel streams consisting of pure CH_4, C_2H_6, C_3H_8 or C_2H_4. These fuels allowed comparisons of results between CH_4 and C_2H_4 and between C_2H_4 and C_2H_6 to separately investigate effects of changing only the number of carbon or hydrogen atoms, and comparisons of results between CH_4, C_2H_6 and C_3H_8 to investigate the effects of simultaneously changing the number of carbon and hydrogen atoms. Collectively those results addressed key aspects of a wide range of practical combustible materials. For the twelve fuel and suppressant combinations, the extinction strain rates were measured at up to four different suppressant concentrations. A substantially higher suppressant effectiveness was observed in the C_2H_4 flames than in previous measurements[21] of wet-CO flames, consistent with the role of H-radical concentrations in the flame extinction process and the suppressant effect in reducing peak levels of H-radicals. Measured extinction strain rates for all fuels and suppressants were found to correlate well with peak temperature just below the extinction limit. However, substantially better correlation was found with the peak value of H-radical concentration, and with corresponding concentrations of H+OH and H+O radicals, especially for the alkane fuels.

These previous studies of chemically-passive fire suppressant effectiveness on hydrocarbon-air diffusion flames were conducted in normal atmospheres. As noted above, with regard to spacecraft environments it is essential to understand the effect of EVA-like atmospheres corresponding to enriched oxygen concentrations and reduced pressures on the relative suppressant effectiveness. The present study thus extends the earlier results in Refs. 20 and 21 to the current standard EVA atmosphere consisting of 30% oxygen in nitrogen at 0.7 bar pressure. In particular, we first extend the earlier normal-atmosphere results for the effect of suppressant concentration on the critical flame extinction strain rate by comparing experimentally measured values with computed results from OPPDIF calculations with the GRI-Mech 3.0 reaction mechanism as well as with computed results from the simple model of Puri and Seshadri[19]. Following this, we focus on the C_2H_6 fuel and use OPPDIF calculations to examine the changes in the internal flame structure due to the presence of each chemically-passive suppressant type for both normal and EVA atmospheres. In particular, based on the earlier correlations[20,21] we compare results for the temperature, major species and minor species concentrations at normal and EVA atmospheres to identify the effect of the enriched oxygen concentration and reduced pressure in the EVA atmosphere on the suppressant effectiveness.

II. Experiments

A. Apparatus

A stable, planar, laminar, opposed-flow diffusion flame was established at the center of an 8-mm-wide vertical gap separating the exit planes of a lower fuel tube and an upper oxidizer tube. The fuel and oxidizer each issued through central tubes having an inner diameter of 10.3 mm, a wall thickness of 0.4 mm, and a length of 200 mm. The diffusion flame was positioned at the center of the vertical gap by adjusting the momentum of the fuel and oxidizer streams. The fuel and oxidizer streams were each surrounded by an annular coflowing nitrogen stream that issued from a coaxial outer tube having an inner diameter of 18.3 mm and a wall thickness of 0.4 mm. The coflowing nitrogen stream velocities were each matched to the respective fuel and oxidizer stream velocities. The nitrogen coflow eliminated entrainment into the fuel and oxidizer streams and minimized disturbances from the surrounding environment. To smooth the velocity profiles issuing from the tubes, each of the two inner tubes contained two 25-mm-long honeycomb flow straighteners having 1.6 mm cell size and located 70 mm and 140 mm upstream of the exit. The fuel, oxidizer and nitrogen streams were metered and controlled using pressure regulators and precision rotameters that had been calibrated with either wet-test or bubble flow meters.

B. Procedures

The hydrocarbon fuels were supplied from high-purity cylinders of methane, ethane, ethylene or propane. The oxidant stream consisted of mixtures of air and suppressant (Ar, N_2 or CO_2) supplied from commercially-prepared high-pressure cylinders premixed to 0%, 10%, 20% or 30% suppressant by volume in order to minimize variability from oxidizer mixture blending by in-line flow metering. For each fuel and suppressant type, the suppressant concentrations investigated are listed in Table 1. Prepared cylinders of air mixed with suppressant allowed the fuel and oxidant flow rates to the opposed-flow diffusion flame to be gradually increased until the extinction strain rate was reached, while at the same time keeping the oxidant mixture composition constant and maintaining the flame position at the center of the gap. The fuel and oxidizer flow rates at the extinction limit, together with the 8 mm gap width, determined the extinction strain rate a_q[22].

Fuel Type	Suppressant	X_S
CH_4	Ar	0, 0.1, 0.2, 0.3
	N_2	0, 0.1, 0.2
	CO_2	0, 0.1
C_2H_4	Ar	0, 0.1, 0.2, 0.3
	N_2	0, 0.1, 0.2, 0.3
	CO_2	0, 0.1, 0.2
C_2H_6	Ar	0, 0.1, 0.2, 0.3
	N_2	0, 0.1, 0.2, 0.3
	CO_2	0, 0.1, 0.2
C_3H_8	Ar	0, 0.1, 0.2, 0.3
	N_2	0, 0.1, 0.2, 0.3
	CO_2	0, 0.1

Table 1. Test conditions for hydrocarbon fuels. X_S = Mole fraction of suppressant.

III. Flame Calculations

Flame calculations were used in the present study in two ways. First, measured values of the critical flame extinction strain rates were compared with calculated values to determine the accuracy with which such calculated values can predict suppressant effectiveness. The calculated values were obtained for all four fuels from the OPPDIF code, and additional values were obtained for ethane and propane fuels using the simple analytical model of Puri and Seshadri[19]. The former allows detailed representations of the chemical kinetics and transport properties across the flame, but does not provide direct parametric insights. The latter involves various simplifying approximations, but in principle allows direct insights into suppressant effects on various parameters that determine the extinction strain rate.

A. Detailed Flame Extinction Strain Rate Calculations

For each case in Table 1, the extinction strain rates were calculated using the OPPDIF one-dimensional opposed-flow diffusion flame code[23]. The CHEMKIN package was used to evaluate chemical reaction rates and thermodynamic and transport properties. The GRI-Mech 3.0 detailed chemical reaction mechanism, consisting of 325 elementary reactions involving 53 species, was used. Although this mechanism has been optimized for methane, it was used without modification for the present fuels. Selected cases were computed separately both with and without the optically-thin radiation model. Results indicated that radiation losses were negligible for the present conditions, and thus all of the computed results included herein are from radiation-free calculations.

To allow comparisons between calculated and measured values for the extinction strain rates a_q, the strain rate in the calculations was defined from the maximum absolute value of the velocity gradient on the oxidizer side; note that this is also the point where the temperature starts to increase sharply. The resulting strain rate values are consistent with the essentially uniform velocity gradient that results from OPPDIF across the interior of the gap for the corresponding nonreacting case[24]. This way of defining the strain rate is also consistent with the widely used choice of the velocity gradient immediately ahead of the preheat zone on the oxidizer side[25,26].

B. Simplified Approximate Calculations of Extinction Strain Rates

Critical flame extinction strain rates were also calculated for ethane and propane flames using the simple analytical model of Puri and Seshadri[19] based on the asymptotic theory developed by Liñan[11] and Peters[12]. This model is based on a one-step overall irreversible chemical reaction between the fuel and oxidizer, and assumes unity Lewis number and unity concentration exponents as well as high activation energy asymptotics and large Damköhler number. Under these assumptions, the critical flame extinction strain rate a_q is calculated from

$$ln\left[a_q \frac{F}{T_{st}^{\,5}} \right] = -\frac{T_a}{T_{st}} + \ln K \qquad (1)$$

where

$$F = \frac{Z_{st}\left[1+\tau\left(1-Z_{st}\right)\right]Y_{F,1}^2}{\left(1-Z_{st}\right)^2 C_p^3}\exp\left[-2\left(erf^{-1}\left[2Z_{st}\right]\right)^2\right] \tag{2}$$

and

$$K = \frac{4\pi\rho_2 T_2 \nu_F^3 M_F^2 B \nu_O}{T_a^3\left(-\Delta h\right)^3 e} \tag{3}$$

$$Z_{st} = \frac{Y_{O,2}}{\left(\nu_O M_O Y_{F,1}/\nu_F M_F\right)+Y_{O,2}} \tag{4}$$

Equation (1) is solved for a_q from known values of the stoichiometric temperature T_{st}, the activation temperature T_a, and the parameters F and K from (2) and (3), respectively. The latter involve the stoichiometric mixture fraction Z_{st} and various properties of the fuel and oxidizer streams. In addition, (3) also requires a value for the pre-exponential factor B in the assumed overall one-step Arrhenius rate equation. This value of B was estimated from the concentrations of fuel and oxidizer in the plane of maximum temperature from the OPPDIF calculations. The reaction rate was then calculated in moles/cm-sec for each fuel using the one-step rate constants from Westbrook and Dryer[27] with an activation energy of 30 kcal/mole. The resulting calculated reaction rate was then equated to an Arrhenius rate, involving B, for the same activation energy and for the fuel and oxidizer concentrations at the plane of maximum temperature.

IV. Results and Discussion

A. Flame Extinction Strain Rates

Flame extinction strain rates a_q were measured for the four hydrocarbon fuels CH_4, C_2H_4, C_2H_6, and C_3H_8 and for the three chemically-passive suppressants Ar, N_2 and CO_2 at each of the concentrations shown in Table 1. For each fuel and all suppressants, the critical extinction strain rate decreased with increasing suppressant concentration. Figure 1 shows the effect of varying the suppressant type on the measured extinction strain rate for a given fuel, in this case showing results for the C_2H_6-flames. Corresponding results for the other fuels were qualitatively similar, though the extinction strain rate at zero suppressant concentration, here denoted a_{q0}, depends on the particular fuel. For all these fuels, the relative suppressant effectiveness $1 - (a_q/a_{q0})$, which gives the fractional reduction in the extinction strain rate relative to the unsuppressed value, increased in order from Ar to N_2 to CO_2, with the latter being the most effective. The observed ordering from the monatomic to the triatomic suppressant is consistent with the simple increase in the specific heat of the non-fuel gases per unit oxygen concentration in a stoichiometric mixture of the fuel and oxidizer streams. Huggett[28] has shown that a wide variety of fuels will not burn in oxygen-containing atmospheres if the heat capacity per gmol of oxygen in the atmosphere exceeds a critical value. This specific heat effect is also consistent with previous observations of suppressant type and concentration on laminar burning velocities of premixed flames[29,30]. In the present diffusion flames, the increased specific heat due to the suppressant leads to a corresponding reduction of the reaction zone temperature in these flames. This in turn contributes to an associated decrease in the reaction rates, and thereby leads to a reduction in the strain rate at which extinction occurs.

Figure 2 shows the effect of varying the fuel type for a given suppressant, with results shown for Ar, N_2 and CO_2 as the suppressants. For each suppressant and for any given concentration of the suppressant, the measured extinction strain rates show the flames to become increasingly more difficult to extinguish in order from CH_4, C_3H_8, C_2H_6 to C_2H_4, with the latter having the highest extinction strain rate. This ordering is consistent with the relative reactivity of each fuel as characterized by its peak laminar burning velocity in a corresponding unsuppressed premixed flame. Ethylene has the highest laminar burning velocity among these fuels, and methane the lowest. Moreover among the alkane fuels a further indication of the relative reactivity is given by the inverse of the ignition temperature, which increases in order from CH_4 to C_3H_8 to C_2H_6[31,32].

The effect of changing from the normal atmosphere (21% O_2 in N_2 at 1 atm pressure) to the EVA atmosphere (30% O_2 in N_2 at 0.7 atm pressure) is shown in Fig. 3, where results are presented for the C_2H_6 and C_3H_8 fuels and for each of the three chemically-passive suppressant types. The EVA conditions have been studied here via the

OPPDIF calculations, and thus the key interest in each of the panels of Fig. 3 is in comparing the dashed line, giving the calculated normal-atmosphere results, with the dot-dashed line, which gives the corresponding EVA-atmosphere results. What is shown by these lines are the calculated strain rates when both flames are operated at the nominal conditions corresponding to the extinction strain rates at normal atmosphere from the experiment. It is apparent that for both fuels and for all three suppressants, slightly lower strain rates are obtained in the EVA-atmosphere flames than in the normal-atmosphere flames at the same operating conditions. The only exception is the propane fuel for the highest concentration of CO_2 suppressant, though since no similar effect is seen for the ethane fuel it remains to be determined if this effect is real. For all other cases, the lower strain rate in the EVA atmosphere suggests that the flames are somewhat more difficult to extinguish in the EVA atmosphere. The O_2-enrichment of the EVA atmosphere leads to an increase in the peak flame temperature, which by itself would be expected to produce an increase in the extinction strain rate. However, the reduced pressure of the EVA atmosphere by itself would be expected to produce a reduction in the mass burning rates, and thus a decrease in the extinction strain rate. The results in Fig. 3 suggest that these two competing effects will largely offset each other, since the net difference found in the strain rates in the normal and EVA atmospheres is relatively small. However, the effect of the increased temperature appears to be dominant, since the net effect is a slight reduction in the strain rate for the same operating conditions, and thus a slight increase in the nominal operating strain rate needed to achieve extinction. It may be possible to obtain improvements in the suppressant effectiveness of spacecraft environments through changes in the pressure and corresponding changes in the O_2 concentration, though this has not been examined here.

The symbols in Fig. 3 give corresponding experimentally measured values of the extinction strain rates at normal-atmosphere conditions for each case. These may be compared with the respective calculated results from OPPDIF. The decrease in the extinction strain rate with increasing suppressant concentration is the same in the measured and calculated results, as are the relative differences between the two fuels for any given suppressant type and concentration. Similarly, the relative differences between the various suppressant types for both fuels and all suppressant concentrations are also similar in the measured and calculated results. However, there are substantial differences in the absolute values of the strain rates obtained from the experiments and from the calculations. It is unlikely that these differences reflect any shortcomings in the chemical kinetic mechanism used in the OPPDIF calculations, or in the transport modeling inherent in the OPPDIF calculations. Instead, these differences between the computed and measured results are more likely due to small differences in the flow field assumed in OPPDIF and that actually obtained in the experiments, and due to the fact that strain rate values in the experiments were obtained indirectly from the fuel and oxidizer stream exit conditions via the simplified formulation of Seshadri and Williams[22]. As a consequence, absolute comparisons between the measured and OPPDIF-calculated values are not directly meaningful. However the fact that the experiments and OPPDIF calculations produce essentially the same trends noted above with fuel type, suppressant type, and suppressant concentration suggests that both sets of results are appropriate for the flow field that applies to each of them.

In order to obtain additional parametric insights into the mechanisms by which the fuel type, the suppressant type, the suppressant concentration, and the oxidizer composition (normal atmosphere vs. EVA atmosphere) influences the suppressant effectiveness, the solid lines in Fig. 3 also show the extinction strain rates obtained via equations (1)-(4) from the simplified approximate formulation of Puri and Seshadri[19]. It appears in Fig. 3 that the a_q values obtained from this approach more closely follow the experimentally measured values than do the corresponding results from the more detailed OPPDIF calculations. However, it must be borne in mind that the experimental values for the strain rates were not measured directly, but instead were estimated from the fuel and oxidizer stream exit conditions using this same approximate formulation. Thus the better agreement between the measured extinction strain rates and those obtained from the formulation in equations (1)-(4) results simply from this fact, and does not indicate that the approximate formulation in Ref. 19 is superior to the highly detailed chemical kinetic and transport modeling in OPPDIF.

Nevertheless, the simplified approximate formulation in equations (1)-(4) does more readily allow parametric insights into the mechanisms by which such chemically-passive suppressants affect the extinction strain rate a_q. In particular, the effects of the fuel type, suppressant type, suppressant concentration, and oxidizer composition on a_q may be inferred from equations (1)-(4) via their respective effects on the stoichiometric mixture fraction Z_{st}, the stoichiometric flame temperature T_{st}, and activation temperature T_a, and the other parameters in this formulation. As a result, this should allow determination of the comparative suppressant effectiveness for other fuel types, other suppressant types, and other oxidizer compositions for terrestrial as well as spacecraft fire safety applications.

B. Flame Structure

To obtain further insights into the fundamental mechanisms by which chemically-passive fire suppressants affect the extinction strain rates of opposed-flow diffusion flames, and in particular into the differences between normal-atmosphere and EVA-atmosphere conditions, the OPPDIF calculations were used to examine the internal structure of each of these flames. Particular attention was focused on the relative roles of the peak flame temperature and the peak values of key radicals across the flame. Figure 4 thus compares the structure of the unsuppressed flames in normal and EVA atmospheres at the same strain rate (a = 100 s^{-1}), in each case showing profiles of major species (C_2H_6, O_2, CO_2, H_2O, CO and C_2H_2) and temperature across the flame in the left panel, and profiles of radical species (H, O and OH) in the right panel. All profiles are shown as functions of the distance from fuel stream exit plane. Results are presented for ethane fuel, however based on the findings in Figs. 2 and 3 the trends are expected to be similar for the other hydrocarbon fuels. It can be seen that the net effect of the reduced pressure and enriched O_2 concentration in the EVA atmosphere is a net increase in the peak flame temperature, from about 1940 K in the normal atmosphere to about 2260 K in the EVA atmosphere. The higher flame temperature leads to increased concentrations of H, O, and OH radicals in the EVA atmosphere. Figure 3 suggests that the net effect will be only a small increase in the extinction strain rate when the normal atmosphere is replaced by the EVA atmosphere.

The results in Fig. 4 provide the baseline flame structure when no suppressant is present in either flame. Figures 5-7 examine the effect of suppressant type on each flame by presenting comparisons of the flame structure at the same 100 s^{-1} strain rate when 20% molar concentration of monatomic (Ar), diatomic (N_2) and triatomic (CO_2) suppressant is introduced in the oxidizer stream. Note that the a = 100 s^{-1} strain rate imposed on all these flames corresponds to a value just below the critical extinction limit for the 20% CO_2-suppressed flame. Note also that maximum concentrations of HO_2 and H_2O_2 radical were found to be roughly three order of magnitude smaller than the concentrations of the OH, H and O radicals shown here. As a result, the latter tend to dominate the relative reactivity in the present flames.

Several trends of particular significance can be seen by comparing Figs. 4-7. First, for the normal-atmosphere flame there is a progressive reduction of the peak flame temperature from 1937 K without suppressant, to 1778 K, 1706 K and 1557 K when 20% concentration of the monatomic, diatomic and triatomic suppressants, respectively, is introduced in the oxidizer. This reduction is principally due to the simple effect of the specific heat of these suppressants, which increase in order from Ar to N_2 to CO_2. The reduction in peak flame temperature with suppressant type is consistent with the decrease in extinction strain rate seen in Fig. 1 for a fixed suppressant concentration. Second, a similar reduction in peak flame temperature with suppressant type can be seen in Figs. 4-7 for the EVA-atmosphere flame, though as expected the absolute temperatures are higher due to the higher oxygen concentrations. This is also consistent with the decrease in strain rate seen for the EVA atmosphere in Fig. 3 for a fixed suppressant concentration. Third, with regard to the radical species it is well known that H, O, and OH radicals play key roles in the chain-branching and chain-terminating reactions that ultimately determine the extinction strain rate in flames. The effect of the oxidizer composition and the suppressant type and concentration in altering these radical concentrations may provide additional insights into the relative effectiveness of any given suppressant beyond its simple influence on the peak flame temperature. Of course, these radical concentrations can be expected to decrease with decreasing peak flame temperature, and direct evidence of this can be see in Figs. 4-7. In both the normal-atmosphere and EVA-atmosphere results, the OH concentrations are more dramatically reduced than the O and H concentrations. In particular, comparing Figs. 4-7 shows that in the normal atmosphere the peak OH radical concentration without suppressant is substantially higher than the peak H radical concentration, while at 20% concentration of any suppressant the peak OH and H concentrations have become nearly the same. At the same time, the relative H and O concentrations have remained largely invariant. A similar comparison of the EVA-atmosphere results shows that the peak OH concentrations is somewhat reduced when any suppressant is added to the oxidizer, but the peak values always remain substantially above the peak H-radical concentration.

V. Conclusions

An opposed-flow diffusion flame configuration has been used to investigate effects of chemically-passive fire suppressants on the strain rate needed to extinguish hydrocarbon flames of pure CH_4, C_2H_6, C_3H_8 or C_2H_4 burning with an oxidizer stream consisting of normal air or EVA atmosphere containing 0-30% volume fraction of Ar, N_2 or CO_2 as inert suppressants. Results show that for all fuels these suppressants perform in order of increasing effectiveness from argon to nitrogen and carbon dioxide, consistent with the increase in specific heat due to the

resulting suppressant concentration in a stoichiometric mixture of the fuel and oxidizer streams. A substantially higher suppressant effectiveness is observed in the present C_2H_4, consistent with the role of H-radical concentrations in the flame extinction process and the suppressant effect in reducing peak levels of H-radicals. The effect of changing from the normal atmosphere (21% O_2 in N_2 at 1 atm pressure) to the EVA atmosphere (30% O_2 in N_2 at 0.7 atm pressure) suggests a slight increase in the strain rate needed to extinguish the present fuels. The O_2-enrichment of the EVA atmosphere leads to an increase in the peak flame temperature, while the reduced pressure of the EVA atmosphere leads to a net reduction in the mass burning rates, with the net effect apparently being a small increase in the extinction strain rate. This suggests that it may be possible to obtain improvements in the suppressant effectiveness of spacecraft environments through changes in the pressure and corresponding changes in the O_2 concentration.

The present experiments and corresponding OPPDIF calculations were found to produce essentially the same trends in extinction strain rate with fuel type, suppressant type, and suppressant concentration. Differences in the absolute values of the strain rates from the experiments and OPPDIF calculations reflect small differences in the flow field assumed in OPPDIF and that actually obtained in the experiments, and due to the fact that strain rate values in the experiments were obtained indirectly from the fuel and oxidizer stream exit conditions via the simplified formulation of Seshadri and Williams[22]. The latter is a simplified approximate formulation that leads to equations (1)-(4), which allow parametric insights into the mechanisms by which such chemically-passive suppressants affect the extinction strain rate a_q. In particular, the effects of the fuel type, suppressant type, suppressant concentration, and oxidizer composition on a_q may be inferred from equations (1)-(4) via their respective effects on the stoichiometric mixture fraction Z_{st}, the stoichiometric flame temperature T_{st}, and activation temperature T_a, and the other parameters in this formulation. As a result, this should allow determination of the comparative suppressant effectiveness for other fuel types, other suppressant types, and other oxidizer compositions for terrestrial as well as spacecraft fire safety applications.

Acknowledgements

This research was supported by NASA Grant No. NNC04GA94G, with Dr. F. Takahashi of NASA Glenn Research Center serving as program manager.

References

[1] Anderson, S.O., *Fire J.,* Vol. 81, 1987, pp. 56-118.

[2] Gann, R.G. (Ed.), *Halogenated Fire Suppressants*, Volume 16, ACS Symposium Series, American Chemical Society, Washington, D.C., 1975.

[3] Biordi, J.C., Lazzara, C.P., Papp, J.F., "Molecular Beam Mass Spectrometry Applied to Determining the Kinetics of Reactions in Flames; I. Empirical Characterization of Flame Perturbation by Molecular Beam Sampling Probes" *Combust. Flame,* Vol. 23, No. 1, 1974, pp. 73-82.

[4] Westbrook, C.K., *Combust. Sci. Technol.,* Vol. 34, 1983, pp. 201-225.

[5] Safieh, H.Y. , Van Drooren, J., Van Tiggelen, P.J., "Experimental Study of Inhibition Induced By CF_3BR In a CO-H_2-Ar Flame", *Proc. Combust. Inst.* Vol. 19, 1982, pp. 117-126.

[6] Sheinsohn, R.S., Penner-Hahn, J.E. and Indritz, D., "The Physical and Chemical Action of The Fire Suppressants", *Fire Safety J.,* Vol. 15, 1989, pp. 437-450.

[7] Linteris, G.T., Truett, L., **"**Inhibition of Premixed Methane-Air Flames by Fluoromethanes", *Combust. Flame,* Vol. 105, No. 1-2, April 1996, pp. 15-27.

[8] Linteris, G.T., Burgess Jr., D.R., Babushok, V., Zachariah, M., Tsang, W. Westmoreland, P., "Inhibition of Premixed Methane–Air Flames by Fluoroethanes and Fluoropropanes" *Combust. Flame,* Vol. 113, No. 1-2, April 1998, pp. 164-180.

[9] Milne, T.A., Green, C.L., Benson, D.K., "The Use of the Counterflow Diffusion Flame in Studies of Inhibition Effectiveness of Gaseous and Powdered Agents" *Combust. Flame*, Vol. 15, No. 3, Dec. 1970, pp. 255-263.

[10] Seshadri, K., Ilinic, N., "The Asymptotic Structure of Inhibited Nonpremixed Methane-Air Flames", *Combust. Flame*, Vol. 101, No. 3, May 1995, pp. 271-286.

[11] Liñan, A., "The Asymptotic Structure of Counterflow Diffusion Flames for Large Activation Energies" *Acta Astronautica*, Vol. 1, 1974, pp. 1007-1039.

[12] Peters, N., "Local Quenching Due to Flame Stretch and Non-Premixed Turbulent Combustion", *Comb. Sci. Technol.* Vol. 30, 1983, pp. 1-17.

[13] Dixon-Lewis, G., Fukutani, S., Miller, J. A., Peters, N., Warnatz, J., "Calculation of The Structure and Extinction Limit of a Methane-Air Counterflow Diffusion Flame in The Forward Stagnation Region of a Porous Cylinder", *Proc. Combust. Inst.* Vol. 20, 1985, pp. 1893-1904.

[14] Tsuji, H., "Counterflow Diffusion Flames", *Prog. Energy Combust. Sci.* Vol. 8, 1982, pp. 93-119.

[15] Tsuji, H., Yamaoka, I., "The Structure of Counterflow Diffusion Flames in the Forward Stagnation Region of A Porous Cylinder", *Proc. Combust. Inst.* Vol. 12, 1969, pp. 997-1005.

[16] Tsuji, H., Yamaoka, I., "Structure Analysis of Counterflow Diffusion Flames in the Forward Stagnation Region of A Porous Cylinder", *Proc. Combust. Inst.* Vol. 13, 1971, pp. 723-731.

[17] Kaoru, M., Youshida, M., Guo, H., Ju, Y., Nhoka, T., "Extinction of Low-Stretched Diffusion Flame in Microgravity" *Combust. Flame*, Vol. 112, No. 1-2, Jan. 1998, pp. 181-187.

[18] Ishizuka, S., Tsuji, H., "An Experimental Study of Effect of Inert Gases on Extinction of Laminar Diffusion Flames", *Proc. Combust. Inst.* Vol. 18, 1981, pp. 695-703.

[19] Puri, I. K., Seshadri, K., "Extinction of Diffusion Flames Burning Diluted Methane and Diluted Propane in Diluted Air", *Combust. Flame,* Vol. 65, No.2, Aug. 1986, pp. 137-150.

[20] Shebl, K.M., Abdelghanie, A.M., Dahm, W.J.A., Faeth, G.M., "Extinction of Nonpremixed Opposed-Flow Hydrocarbon Flames by Chemically-Passive Fire Suppressants", *Proc. Combust. Inst.,* 2006, submitted for publication.

[21] Shebl, K.M., Abdelghanie, A.M., Dahm, W.J.A., Faeth, G.M., "Effects of Chemically-Passive Suppressants on the Extinction of Laminar Nonpremixed Wet Carbon Monoxide Flames", *Combust. Flame*, 2005, submitted for publication.

[22] Seshadri, K., and Williams, F.A., "Laminar Flow Between Parallel Plates With Injection of a Reactant at High Reynolds Number", *Int'l. J. Heat Mass Transfer*, Vol. 21, No. 2, 1978, pp. 251-253.

[23] Kee, R.J., Miller, J.A., Evans, G.H., Dixon-Lewis, G., "A Computational Model of The Structure and Extinction of Strained, Opposed Flow, Premixed Methane-Air Flames", *Proc. Combust. Inst.* Vol. 22, 1988, pp. 1479-1494.

[24] Vagelopoulos, G.M., Egolfopoulos, F.N., "Laminar Flame Speeds and Extinction Strain Rates of Mixtures of Carbon Monoxide with Hydrogen, Methane, and Air", *Proc. Combust. Inst.* Vol. 25, 1994, pp. 1317-1323.

[25] Law, C.K. Zhu, D.L., Yu, G., "Propagation and Extinction of Stretched Premixed Flames", *Proc. Combust. Inst.* Vol. 21, 1986, pp. 1419-1426.

[26] Du, D.X., Axelbaum, R.L., Law, C.K., "Experiments on the Sooting Limits of Aerodynamically-Strained Diffusion Flames", *Combust. Inst.* Vol. 22, 1988, pp. 387-394.

[27] Westbrook, C.K., Dryer, F.L., "Simplified Reaction Mechanisms for Oxidation of Hydrocarbon Fuels in Flames", *Combust. Sci. Technol.,* Vol. 27, 1981, pp. 31-43.

[28] Huggett, C., "Habitable Atmospheres Which Do Not Support Combustion", *Combust. Flame,* Vol. 20, No.1, Feb. 1973, pp. 140-142.

[29] Qiao, L., Kim, C. H., Faeth, G.M., "Suppression Effects of Diluents on Laminar Premixed Hydrogen/Oxygen/Nitrogen Flames", *Combust. Flame,* Vol. 143, No. 1-2, October 2005, pp. 79-96.

[30] Qiao, L., Gu, Y., Dahm, W.J.A., Oran, E., Faeth, G.M., "Near Limit Laminar Burning Velocity of Microgravity Premixed Hydrogen Flames With Chemically-Passive Suppressants", *Proc. Combust. Inst.* (2006), submitted for publication.

[31] Westbrook, C.K., Dryer, F.L., "Chemical Kinetic Modeling of Hydrocarbon Combustion", *Prog. Energy Combust. Sci.*, Vol. 10, 1984, pp. 1-57.

[32] Fotache, C.G., Wang, H., Law, C.K., "Ignition of Ethane, Propane, and Butane in Counterflow Jets of Cold Fuel Versus Hot Air Under Variable Pressures", *Combust. Flame,* Vol. 117, No. 4, June 1999, pp. 777-794.

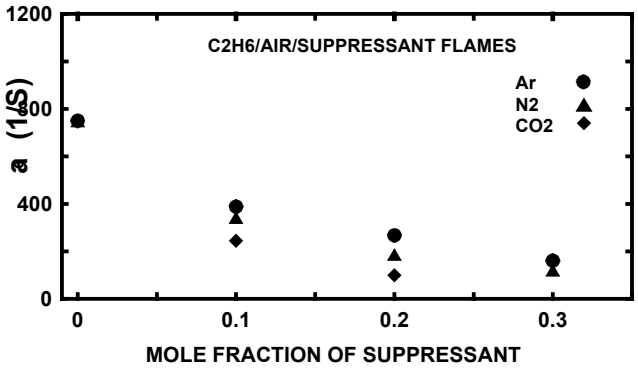

Figure 1. Comparison of measured extinction strain rates for C_2H_6-air opposed-flow diffusion flames in normal atmosphere for varying concentrations of monatomic (Ar), diatomic (N_2) and triatomic (CO_2) suppressants. From Ref. 20.

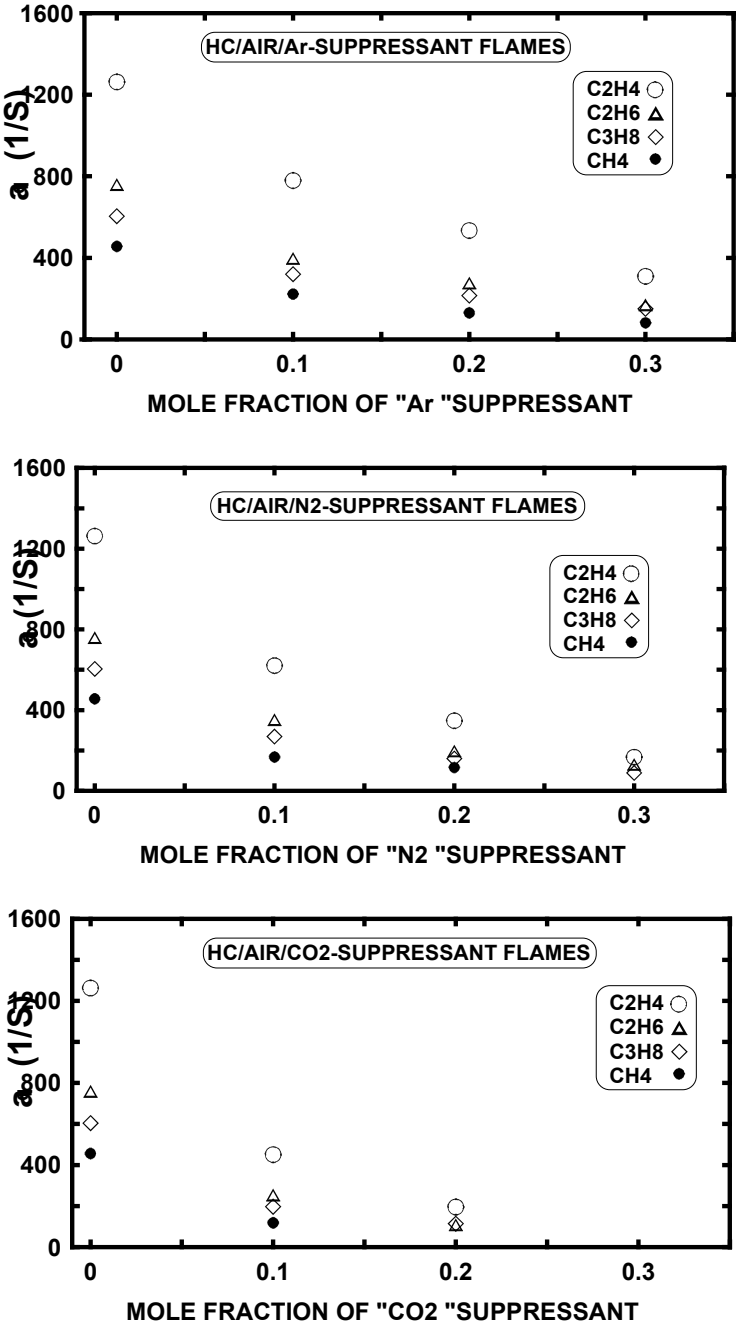

Figure 2. Effectiveness of chemically-passive fire suppressants in normal atmosphere, showing experimentally measured values of the flame extinction strain rate a_q for hydrocarbon-air opposed-flow diffusion flames for the four fuels listed in Table 1. Shown are results obtained for varying concentrations of monatomic (Ar) suppressant *(top)*, diatomic (N_2) suppressant *(middle)*, and triatomic (CO_2) suppressant *(bottom)* in the oxidizer stream. From Ref. 20.

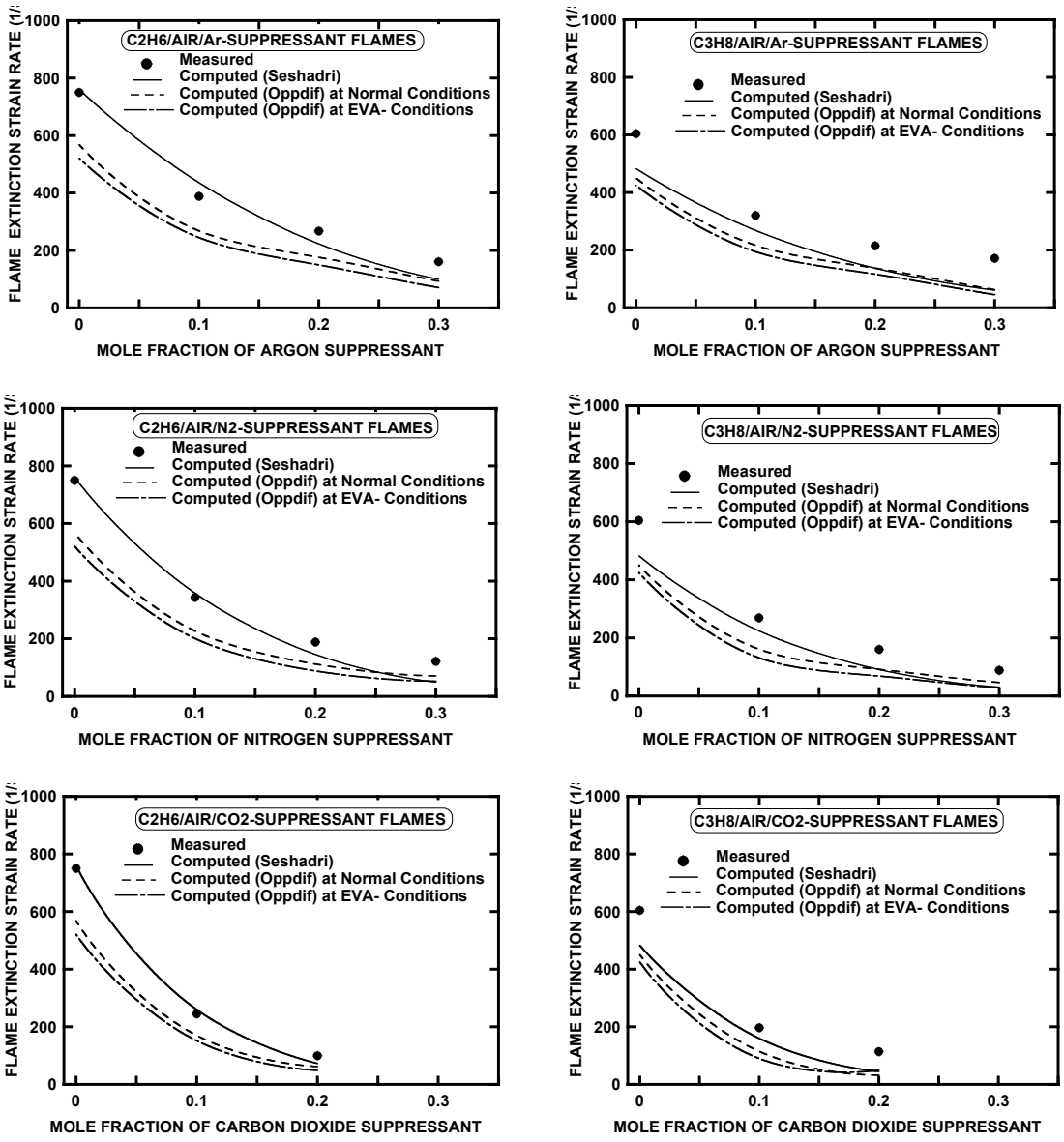

Figure 3. Effectiveness of chemically-passive fire suppressants in normal atmosphere *(dashed line)* and EVA atmosphere *(dot-dashed line)*, showing results from OPPDIF calculations for C_2H_6 flames *(left)* and C_3H_8 flames *(right)* with Ar suppressant *(top row)*, N_2 suppressant *(middle row)* and CO_2 suppressant *(bottom row)*. Also shown are corresponding measured extinction strain rates in normal atmosphere *(symbols)* and simplified calculations using approximate formulation of Puri & Seshadri (1986) *(solid line)* as described herein.

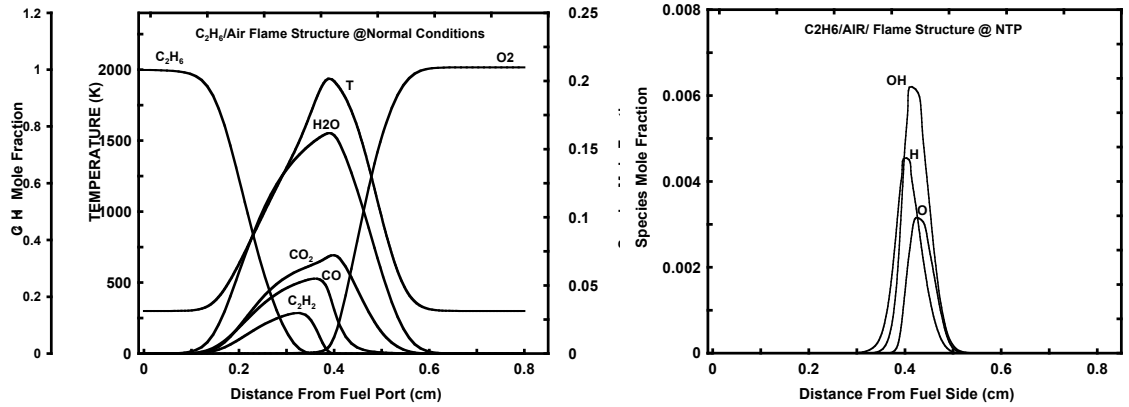

Fig. 4*a*. Normal atmosphere; no suppressant.

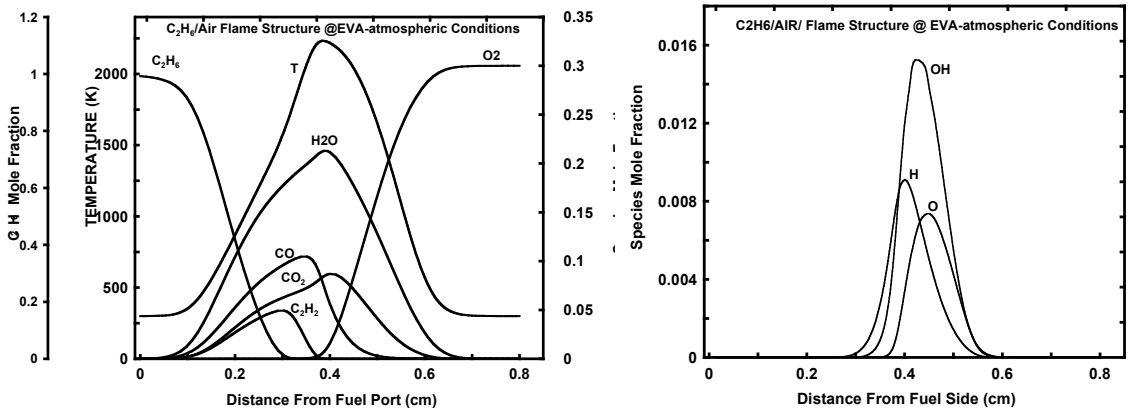

Fig. 4*b*. EVA atmosphere; no suppressant.

Figure 4. Comparison of baseline flame structure for C_2H_6 flames without suppressant in normal atmosphere *(top row)* and in EVA atmosphere *(bottom row)*, showing results from OPPDIF calculations for major species and temperature *(left)* and for key radical species *(right)*. Compare with corresponding results for monatomic, diatomic and triatomic suppressants in Figs. 5, 6 and 7, respectively.

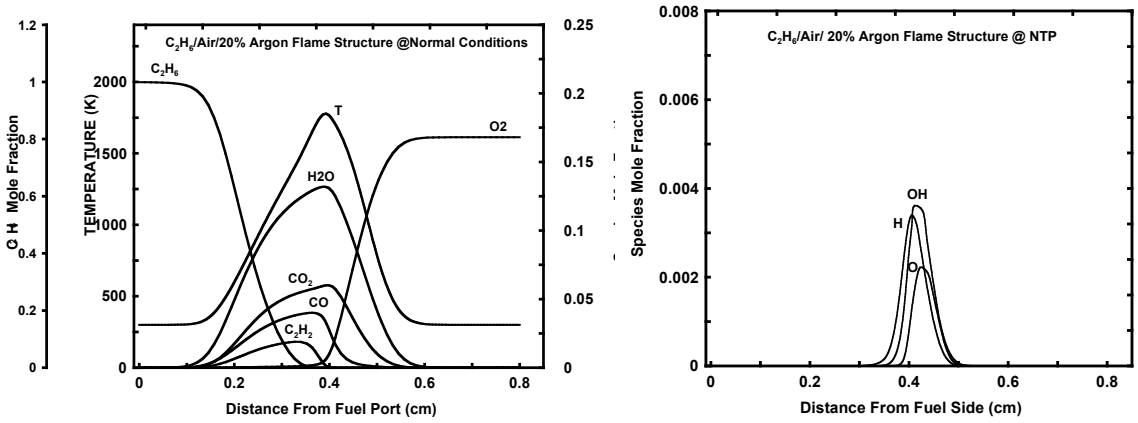

Fig. 5*a*. Normal atmosphere; 20% Ar suppressant.

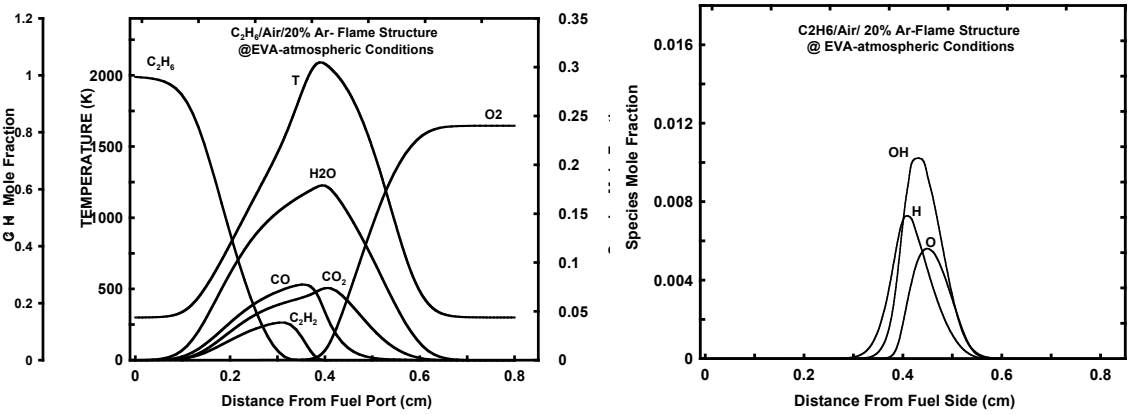

Fig. 5*b*. EVA atmosphere; 20% Ar suppressant.

Figure 5. Comparison of flame structure for C_2H_6 flames with 20% Ar suppressant in normal atmosphere *(top row)* and in EVA atmosphere *(bottom row)*, showing results from OPPDIF calculations for major species and temperature *(left)* and for key radical species *(right)*. Compare with corresponding results for unsuppressed flames in Fig. 4, and for diatomic and triatomic suppressants in Figs. 6 and 7, respectively.

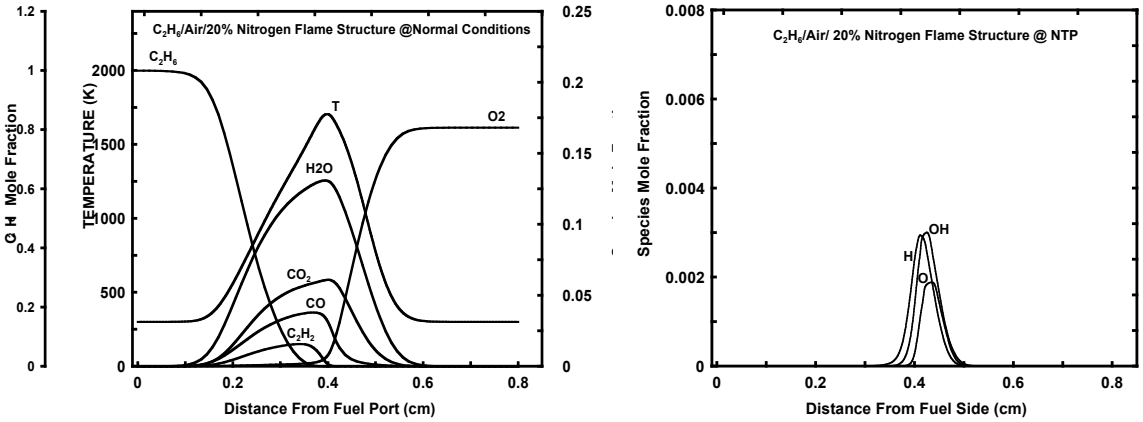

Fig. 6*a*. Normal atmosphere; 20% N_2 suppressant.

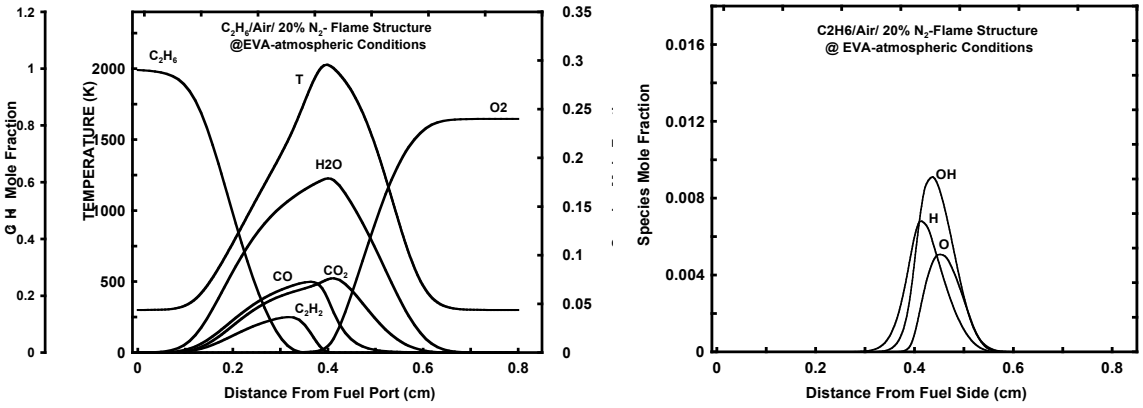

Fig. 6*b*. EVA atmosphere; 20% N_2 suppressant.

Figure 6. Comparison of flame structure for C_2H_6 flames with 20% N_2 suppressant in normal atmosphere *(top row)* and in EVA atmosphere *(bottom row)*, showing results from OPPDIF calculations for major species and temperature *(left)* and for key radical species *(right)*. Compare with corresponding results for unsuppressed flames in Fig. 4, and for monatomic and triatomic suppressants in Figs. 5 and 7, respectively.

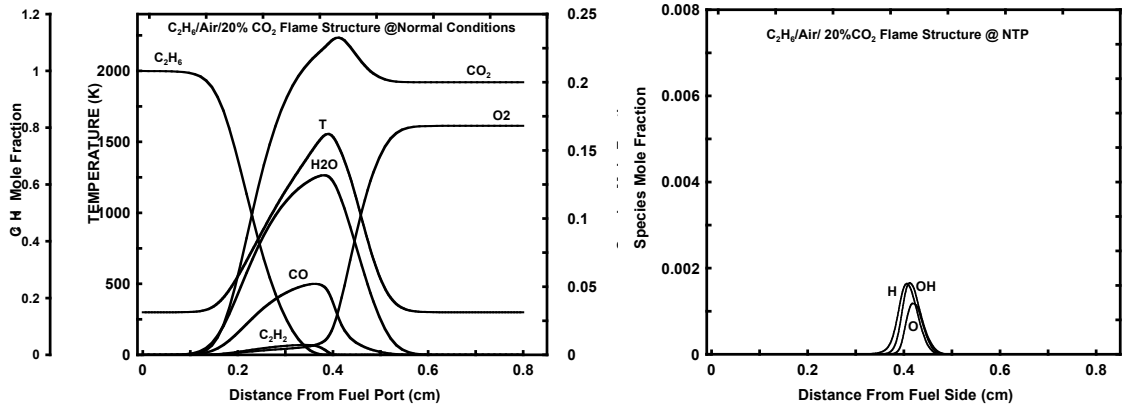

Fig. 7*a*. Normal atmosphere; 20% CO_2 suppressant.

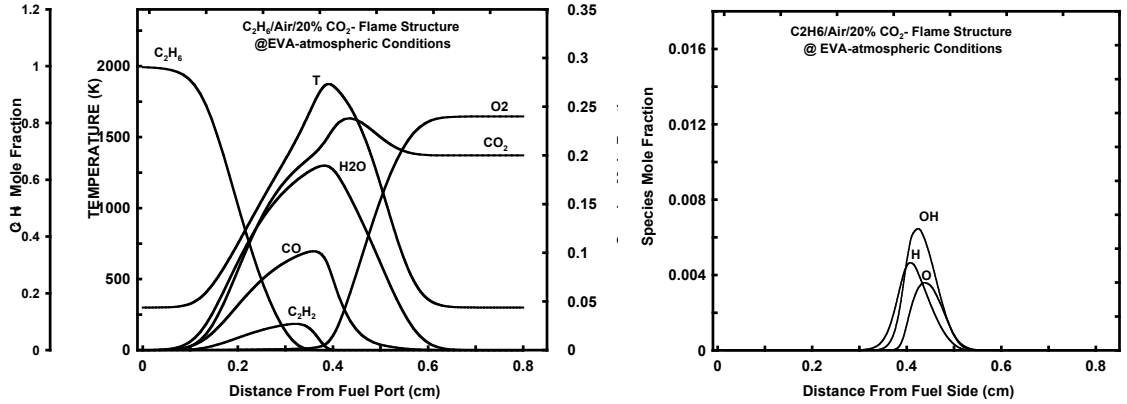

Fig. 7*b*. EVA atmosphere; 20% CO_2 suppressant.

Figure 7. Comparison of flame structure for C_2H_6 flames with 20% CO_2 suppressant in normal atmosphere *(top row)* and in EVA atmosphere *(bottom row)*, showing results from OPPDIF calculations for major species and temperature *(left)* and for key radical species *(right)*. Compare with corresponding results for unsuppressed flames in Fig. 4, and for monatomic and diatomic suppressants in Figs. 5 and 6, respectively.